VNU Journal of Science: Mathematics - Physics

Journal homepage: https://js.vnu.edu.vn/MaP

Original Article

Study on Optical Features of Circular Photonic Crystal Fibers with Various Air-hole Size

Dang Van Trong[1], Le Tran Bao Tran[1], Chu Van Lanh[1], Nguyen Thi Hong Phuong[2], Nguyen Minh Hang Trang[3], Hoang Trong Duc[4], Nguyen Thi Thuy[4,*]

[1]*Vinh University, 182 Le Duan, Vinh City, Vietnam*

[2]*Nguyen Chi Thanh High School, Hoa Thanh, Tay Ninh, Vietnam*

[3]*IGC Tay Ninh High School, Tay Ninh, Vietnam*

[4]*University of Education, Hue University, 34 Le Loi, Hue City, Vietnam*

Received 20 April 2022
Revised 02 June 2022; Accepted 02 June 2022

Abstract: In this workwe proposed a newly designed photonic crystal fiber (PCF) with a circular lattice, the difference between the air-hole diameters of the first ring and the other rings makes it possible to improve the nonlinear properties of fibers. We investigated the effect of varying the filling factor (d_1/Λ) and lattice constant (Λ) on the nonlinear characteristics of photonic crystal fibers in the 0.5 - 2 μm wavelength range. The advantages of these photonic crystal fibers are the flat and near-zero dispersion, low attenuation, and high nonlinear coefficient. From simulation results, we have selected three optimal structures (Λ = 1.0 μm; d_1/Λ = 0.4, Λ = 0.8 μm; d_1/Λ = 0.6, and Λ = 0.8 μm; d_1/Λ = 0.65) to analyze the nonlinear characteristics at the pump wavelengths. The proposed fibers are valuable for supercontinuum generation.

Keywords: Photonic crystal fibers (PCFs), circular lattice, supercontinuum generation (SCG), dispersion.

1. Introduction

In 1996, at the optical fiber conference (OFC) [1], Russell and colleagues announced a new type of optical fiber, the photonic crystal fiber (PCF). PCF is an optical fiber that uses photonic crystals to create a cladding around the core of the fiber. The photonic crystal is a medium made up of cyclically

* Corresponding author.
E-mail address: ntthuy@hueuni.edu.vn

https//doi.org/10.25073/2588-1124/vnumap.4728

arranged micrometer-sized air holes that run along the entire fiber length, and this medium has a cyclically variable dielectric constant and has low loss [2].

Since then, scientists worldwide has focused their researches on PCF, because PCF has superior advantages over conventional optical fibers in design and manufacture [1, 2]. It can be designed flexibly in light guide mechanism, material selection, lattice types, shape and size of air-hole, etc. This gives PCF to have a wide range of applications such as fiber lasers, optical amplifiers, nonlinear devices, highly sensitive sensors, and especially supercontinuum generation (SCG) applications [3-7]. SCG can produce high-intensity continuum light sources, approximating laser light sources for many science engineering applications and technology applications [8]. Nonlinear effects that cause spectral expansion during SCG include self-phase modulation (SPM), Four-wave mixing (FWM), soliton kinetics, unstable modulation, Raman scattering, and dispersion. Furthermore, dispersion, effective mode area, and attenuation are important PCF characteristics that determine the performance of SCG. The dispersion characteristic should be flat and near the zero-dispersion curve, and the effective mode area and total loss should be as small as possible. Up to now, there are many research works on PCF, usually focusing on three main types of PCF lattice including circular lattice [9-10], square lattice [11, 12], and hexagonal lattice [13]. Outstanding results obtained from the above studies include high negative dispersion, low confinement loss, ultra-wide bandwidth, compactness, etc. These works analyzed the influence of the fill factor and lattice constant on the PCF characteristic for each lattice structure, but the optimal level of PCF feature for each type of lattice has not been evaluated yet. Recently, the work [14] has studied the influence of structural parameters on PCF properties for each type of lattice, but the authors have not applied the results obtained in supercontinuum generation. Most authors have not emphasized the role of differences in air-hole diameter in the rings in properties of PCF.

In our work, a newly designed photonic crystal with circular lattice and difference in air-hole diameters in the rings was noticed to control the PCF characteristics. We analyzed the effect of the change in the filling factor (d_1/Λ) of the first ring and the lattice constant (Λ) on the PCF nonlinear properties. From that, three optimal structures (Λ = 0.8 μm; d_1/Λ = 0.6, Λ = 0.8 μm; d_1/Λ = 0.65, and Λ = 1.0 μm; d_1/Λ = 0.4) of PCF have been proposed to consider for the SCG.

2. Numerical Modeling

In this work, we used Lumerical mode solutions software [15] to design a photonic crystal fiber with a circular structure of air-hole eight layers in the photonic cladding, as shown in Figure 1. Fused glass silica was used for the base material. The circular lattices PCF structure was chosen to investigate, because it has better advantages than other lattices including high symmetry, tight light confinement to the core, and increases nonlinearity. This leads to a better SCG efficiency of the circular lattice PCF structure, i.e. better bandwidth enhancement compared to other lattices. In [16], authors analyzed the characteristic quantities and compared the SCG efficiency of photonic crystal fibers in three types of circular, square, and hexagonal lattices. The results show that, although the dispersion obtained in the circular lattice has a flatness in the wavelength range smaller than that of the square and hexagonal lattice, the nonlinear coefficient in the circular lattice structure is the largest and the loss is the smallest. Therefore, the obtained supercontinuum (SC) spectrum bandwidth of the circular lattice is equivalent to that of the other two lattices, but the circular lattice obtains the flattest and smoothest SC spectrum, and the hexagonal lattice has the highest noise. The flat and smooth spectrum helps PCF to have a more stable signal propagating in the fiber in the long-wavelength range when applied experimentally. The first ring (the inner near the core) has an air-hole diameter of d_1, which corresponds to a filling factor of d_1/Λ. Meanwhile, the air-hole diameter in the remaining lattice

rings is *d*, corresponding to the filling factor *d/Λ*. Saitoh et al., [17] have demonstrated that the size of the air-hole in the first ring is the main factor affecting dispersion and the remaining rings affect the attenuation. So, our structures are simulated with filling factor d_1/Λ of 0.3, 0.35, 0.4, 0.45, 0.5, 0.55, 0.6, 0.65, 0.7, 0.75, and 0.8, respectively, while filling factor in the remaining rings is constant with d/Λ = 0.95. This results in minimal attenuation for PCFs and one can control the dispersion to obtain optimal dispersion. The lattice constants selected for the survey are *of* Λ = 0.7 µm, Λ = 0.8 µm, Λ = 1.0 µm, and Λ = 1.5 µm. The core diameter depends on d_1 and the lattice constant (Λ), itsis determined by $D_{core} = 2\Lambda - d_1$. Structural parameters are selected by the technological requirements commonly used for the PCF development.

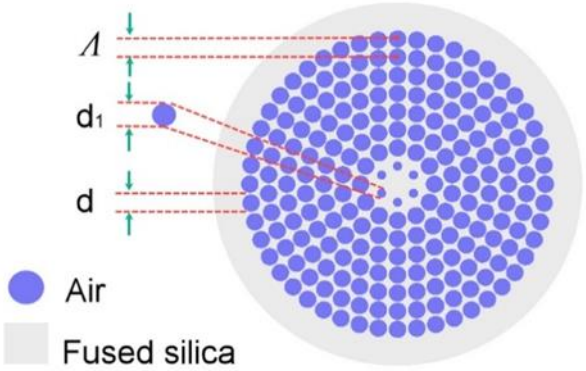

Figure 1. Cross-section of silica-based PCF with circular lattice.

Fiber's dispersion includes a waveguide and material dispersion. It is determined according to Eq. (1), where *Re* $[n_{eff}]$ is the real part of the effective refractive index of a guided mode and *c* is the velocity of light in a vacuum.

$$D = -\frac{\lambda}{c}\frac{d^2\,\mathrm{Re}\left[n_{\mathrm{eff}}\right]}{d\lambda^2} \tag{1}$$

The refractive index of fused silica is obtained using the Smellier equation Eq. (2) [18], which depends on the micrometer-sized wavelength (λ).

$$n^2_{\text{Fused silica}}(\lambda) = 1 + \frac{0.6694226\lambda^2}{\lambda^2 - 4.4801\times10^{-3}} + \frac{0.4345839\lambda^2}{\lambda^2 - 1.3285\times10^{-2}} + \frac{0.8716947\lambda^2}{\lambda^2 - 95.341482} \tag{2}$$

The nonlinear coefficient of PCF has the unit of ($W^{-1}.km^{-1}$) determined by the formula in Eq. (3) [19]:

$$\gamma = \frac{\omega}{c}\left(\frac{n_2}{A_{eff}}\right) = \frac{2\pi}{\lambda}\left(\frac{n_2}{A_{eff}}\right) \tag{3}$$

where, ω is the angular frequency, A_{eff} is the effective mode area (an important characteristic of PCF). It is inversely proportional to the nonlinear coefficient and is defined as in Eq. (4) [19]:

$$A_{\text{eff}} = \frac{\left(\int_{-\infty}^{\infty} \int_{-\infty}^{\infty} |E(x,y)|^2 \, dxdy \right)^2}{\int_{-\infty}^{\infty} \int_{-\infty}^{\infty} |E(x,y)|^4 \, dxdy} \tag{4}$$

where, E is the electric field amplitude.

3. Results and Discussion

Figure 2 illustrates the change in the effective refractive index of the fundamental mode in PCFs with the filling factor (d_1/Λ) chosen between 0.3 and 0.8 and the lattice constant (Λ): Λ = 0.7 µm, Λ = 0.8 µm, Λ = 1.0 µm, and Λ = 1.5 µm. Based on the graph, one can see that the change of wavelength, d_1/Λ, and lattice constant (Λ) lead to the change in the effective refractive index. Specifically, as the wavelength increases, the refractive index decreases, because the penetration of long wavelengths in the mantle is stronger than that of short wavelengths. In addition, as the filling factor (d_1/Λ) increases, the effective refractive index decreases, and n_{eff} increases if the lattice constant (Λ) increases.

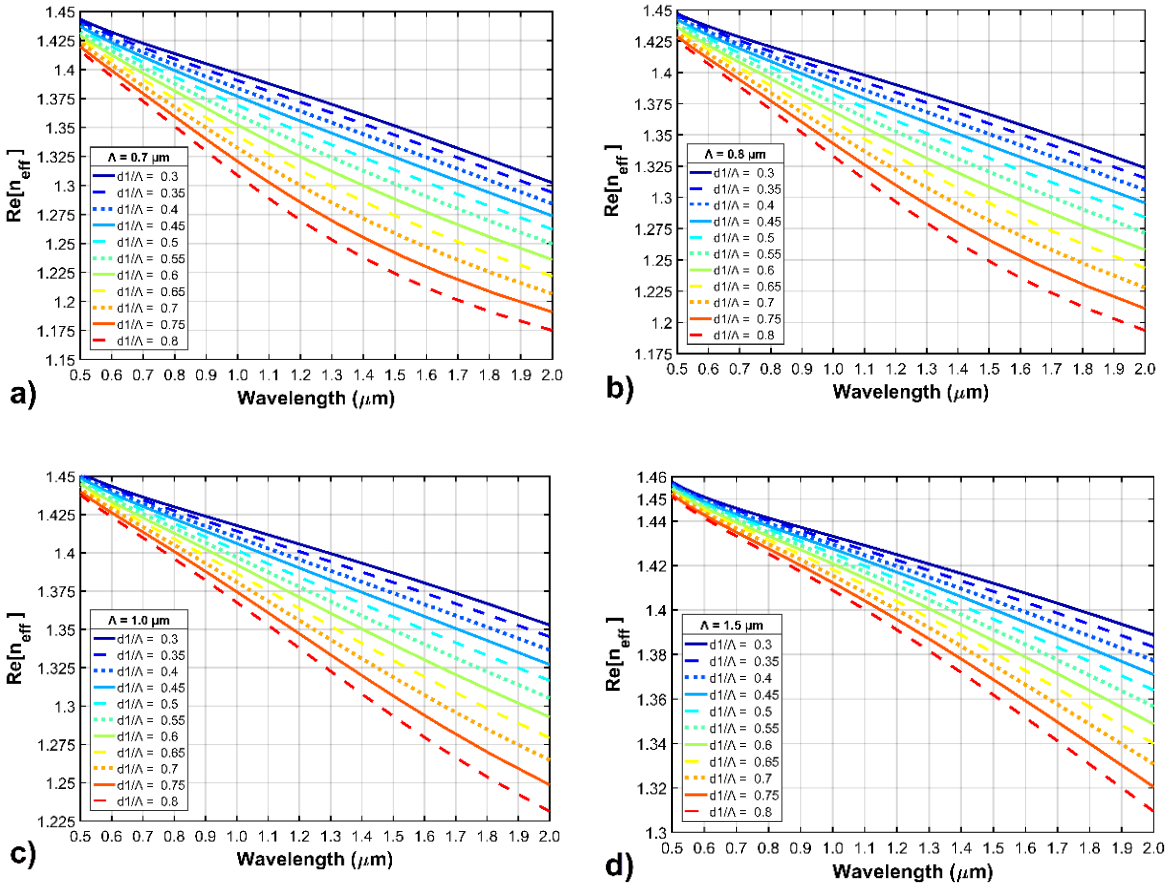

Figure 2. The real part of the effective refractive index as a function of wavelength of PCFs with various d_1/Λ for (a) Λ =0.7 µm, (b) Λ = 0.8 µm, (c) Λ =1.0 µm, and (d) Λ = 1.5 µm.

The value of the real part of the effective refractive index of fibers with different Λ and d_1/Λ at wavelength 1.55 µm can be shown in Table 1. The results show that the effective refractive index of PCFs at the same lattice constant has the maximum value at d_1/Λ = 0.3 and the minimum value at d_1/Λ = 0.8. The value of the maximum effective refractive index of the fiber at wavelength 1.55 µm is 1.41 for the case Λ = 1.5 µm and d_1/Λ = 0.3. From this, one can confirm that the effective refractive index has mainly influenced by the filling factor (d_1/Λ) and the lattice constant (Λ).

Figure 3 shows the dispersion (D) effect of the variaton of filling factor (d_1/Λ) and the lattice constant (Λ). From this figureone can see that the circular lattice structure has dispersion varies with different wavelengths, the dispersion curves obtained include all-normal dispersion (that was not found in some previous works [6, 10, 20]), anomalous dispersion with one or two zero dispersion wavelength (ZDW).

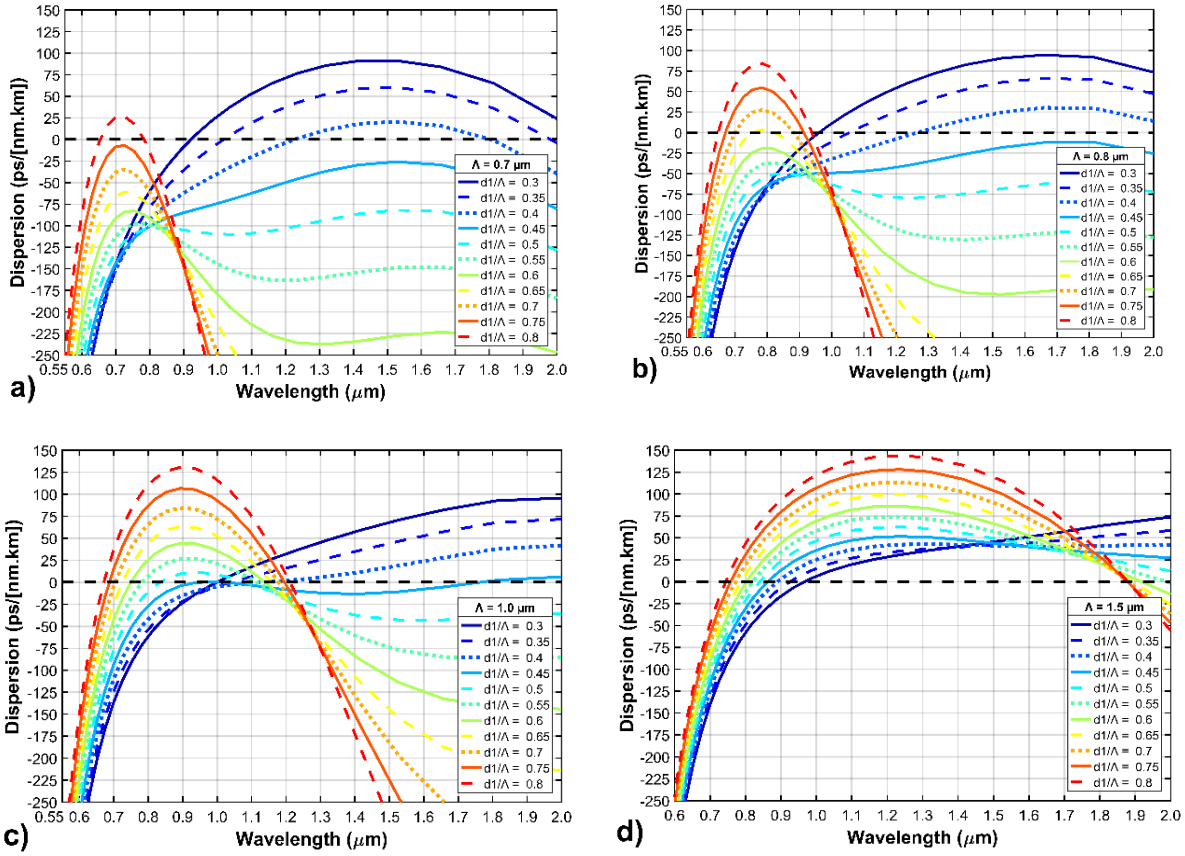

Figure 3. The dispersion as a function of wavelength of PCFs with various d_1/Λ for (a) Λ = 0.7 µm, (b) Λ = 0.8 µm, (c) Λ =1.0 µm, and (d) Λ = 1.5 µm.

The dispersion characteristic has been dominated by the change of the filling factor d_1/Λ and the lattice constant (Λ). Moreover, the change of these two parameters causes the ZDW to shift to a longer wavelength. Specifically, at a lattice constant Λ = 0.7 µm (Figure 3a), anomalous dispersion with one ZDW is only present in fiber with d_1/Λ = 0.3, an all-normal dispersion curve appears as the filling factor increases and is obtained at values of d_1/Λ = 0.45 - 0.75. However, when d_1/Λ = 0.8, an anomalous dispersion curve appears with two ZWDs. It can be seen that the variation of the filling

factor (d_1/Λ) has brought about a variety of dispersion characteristics of the PCFs. At lattice constant Λ = 0.8 μm (Figure 3b) there are four all-normal dispersion curves compared to eight at Λ = 0.7 μm. Furthermore, when investigating at larger lattice constants (larger cores) with Λ = 1.0 μm (Figure 3c) and Λ = 1.5 μm (Figure 3d), the results show that the all-normal dispersion curves no longer appear, but only anomalous dispersion curves with one and two ZWDs in these two cases. The structure parameter Λ also strongly influences the properties of dispersion, a huge change like the dispersion profile observed with a larger lattice constant. The dispersion characteristic is more controllable in smaller core PCFs because of their strong light confinement. From the above analysis, the dispersion characteristics can be controlled through the change of the filling factor (d_1/Λ) of the first ring and the lattice constant (Λ).

Table 1. Real part of the effective refractive index of silica-based PCF at 1.55 μm with lattice constant Λ = 0.7 μm, Λ = 0.8 μm, Λ = 1.0 μm, and Λ = 1.5 μm the filling factor d_1/Λ varies from 0.3 to 0.8.

λ (μm)	d_1/Λ	*Re* [n_{eff}]			
		Λ = 0.7 (μm)	Λ = 0.8 (μm)	Λ = 1.0 (μm)	Λ = 1.5 (μm)
1.55	0.3	1.347	1.362	1.384	1.41
	0.35	1.339	1.355	1.377	1.406
	0.4	1.329	1.346	1.37	1.402
	0.45	1.319	1.337	1.362	1.397
	0.5	1.308	1.327	1.354	1.393
	0.55	1.296	1.315	1.345	1.388
	0.6	1.283	1.303	1.335	1.383
	0.65	1.268	1.29	1.325	1.377
	0.7	1.253	1.275	1.313	1.371
	0.75	1.236	1.26	1.3	1.364
	0.8	1.218	1.242	1.287	1.357

Dispersion is one of the key factors for SCG, the flat dispersion fiber allows for a wider SCG will be obtained. Therefore, fiber structures with flat dispersion curves, near-zero dispersion curves, and ZDWs compatible with pump wavelength have always been the goal of dispersion optimization. Based on preliminary simulations, we proposed three fibers with optimal dispersion with structural parameters as shown in Table 2. They are named as #F_1, #F_2, and #F_3 respectively.

Table 2. The structural parameters of the proposed PCFs

#	Λ (μm)	d_1/Λ	D_{core} (μm)
#F_1	1.0	0.4	1.6
#F_2	0.8	0.6	1.12
#F_3	0.8	0.65	1.08

Figure 5 shows the attenuation characteristic of the basic model for fibers #F_1, #F_2, and #F_3. The attenuation values of the three fibers are all relatively low and there is no large difference in values in the wavelength range of less than 1.7 μm. When the wavelength is greater than 1.7 μm, the attenuation values of #F_2 and #F_3 increase dramatically, but the value of #F_3 is always larger than #F_2. The attenuation is the lowest for the #F_1 fiber and almost coincides with the horizontal axis. The attenuation

values of the proposed fibers #F_1, #F_2, and #F_3 at the pump wavelength are $2.312.10^{-17}$ (dB/m), $-1.187.10^{-18}$ (dB/m), and $3.435.10^{-18}$ (dB/m), respectively. PCFs with minimal attenuation are the advantage of our design.

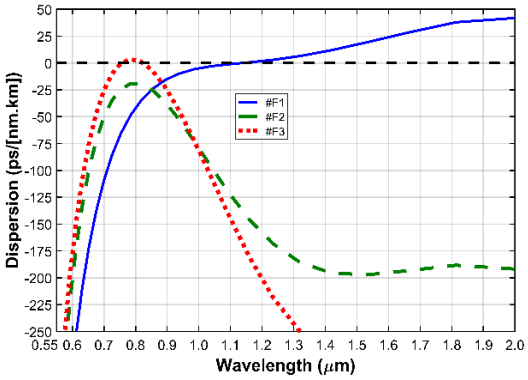

Figure 4. The dispersion properties of the proposed PCFs.

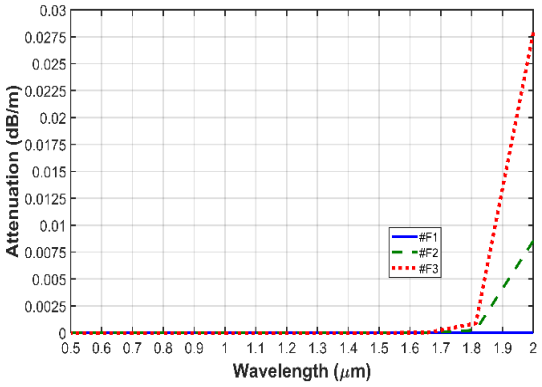

Figure 5. The attenuation properties of the proposed PCFs.

The dependence of the effective mode area and nonlinearity coefficient of the fundamental mode on the wavelength for the #F_1, #F_2, and #F_3 fibers is shown in Figure 6 and Figure 7, respectively. The effective mode area increases with increasing wavelength, and the effective mode area of #F_1 is larger than that of #F_2 and #F_3 on the investigated wavelength range. Furthermore, the effective mode areas of #F_2 and #F_3 are approximately equal each to other, where #F_2 is higher. The effective mode area value at the pump wavelength of #F_1 is 2.949 (μm^2) and that of #F_2, #F_3 with pump wavelength 0.8 μm is 0.982 (μm^2) and 0.89 (μm^2), respectively. From Eq. (3), one can see that the effective mode area is inversely proportional to the nonlinear coefficient. Therefore, the nonlinear coefficient of the #F_1 fiber is the smallest among the three proposed fibers, and the #F_3 fiber has the highest nonlinear coefficient in the studied wavelength range. Besides, the value of nonlinear coefficient at the same pumping wavelength of #F_2, #F_3 is 164.193 (W^{-1}.km^{-1}) and 181.113 (W^{-1}.km^{-1}), respectively, while this value is equal to 54.671 (W^{-1}.km^{-1}) at pump wavelength 1.3 μm for #F_1 fiber.

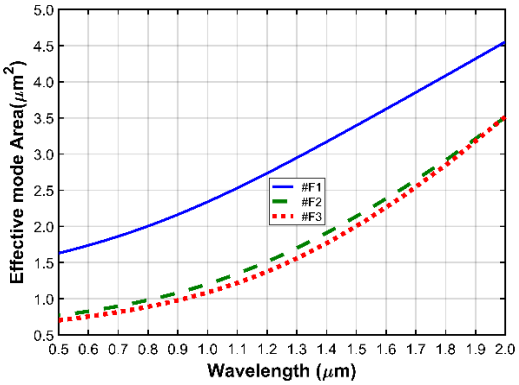

Figure 6. The effective mode area properties of the proposed PCFs.

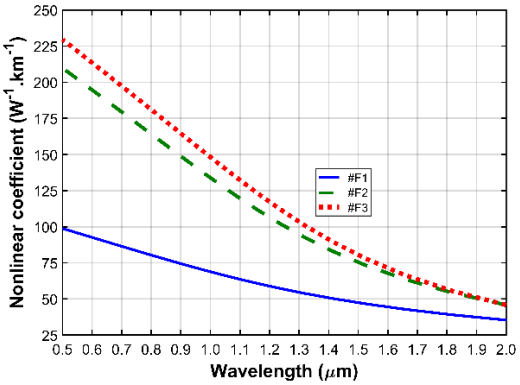

Figure 7. The nonlinear coefficients of the proposed PCFs.

The results obtained from the above analyzes showed that the proposed fibers possess the optimal dispersion, and the values of the characteristics are suitable for the supercontinuum generation.

Table 3. The value of quantities characterizing is calculated at the pump wavelength of the proposed PCFs.

#	the pump wavelength (μm)	D [ps.(nm.km)$^{-1}$]	A_{eff} (μm^2)	γ (W^{-1}.km^{-1})	L_k (dB/m)
#F_1	1.3	5.667	2.949	54.671	$2.312.10^{-17}$
#F_2	0.8	-19.407	0.982	164.193	$-1.187.10^{-18}$
#F_3	0.8	2.53	0.89	181.113	$3.435.10^{-18}$

4. Conclusion

In this work, we have designed a new photonic crystal fiber with differences in the air-hole diameters in the cladding. The characteristic properties of circular lattice PCFs are controlled by varying both the filling factor and lattice constant. The PCFs in our study have outstanding advantages of diverse dispersion, high nonlinear coefficient, and low attenuation. The characteristic properties including the effective mode area, nonlinear coefficient, dispersion, and attenuation of the proposed fibers have also been studied. The proposed fibers have a promising value for the supercontinuum generation.

Acknowledgments

This research is funded by Vietnam National Foundation for Science and Technology Development (NAFOSTED) under grant number 103.03-2020.03 and Vietnam's Ministry of Education and Training (B2021-DHH-08).

References

[1] J. C. Knight, T. A. Birks, P. S. J. Russell, D. M. Atkin, All-silica Single-mode Optical Fiber with Photonic Crystal Cladding, Optics Letters, Vol. 21, No. 19, 1996, pp. 1547-1549, https://doi.org/10.1364/OL.21.001547.

[2] J. C. Knight, Photonic Crystal Fibers, Nature, Vol. 424, 2003, pp. 847-851, https://doi.org/10.1038/nature01940.

[3] C. V. Lanh, H. V. Thuy, C. V. Long, K. Borzycki, D. X. Khoa, T. Q. Vu, M. Trippenbach, R. Buczyński, J. Pniewski, Supercontinuum Generation in Photonic Crystal Fibers Infiltrated with Nitrobenzene, Laser Physics, Vol. 30, No. 3, 2020, pp. 035105, https://doi.org/10.1088/1555-6611/ab6f09.

[4] C. V. Lanh, H. V. Thuy, C. V. Long, K. Borzycki, D. X. Khoa, T. Q. Vu, M. Trippenbach, R. Buczyński, J. Pniewski, Optimization of Optical Properties of Photonic Crystal Fibers Infiltrated with Chloroform for Supercontinuum Generation, Laser Physics, Vol. 29, No. 7, 2019, pp. 075107, https://doi.org/10.1088/1555-6611/ab2115.

[5] D. X. Khoa, C. V. Lanh, H. D. Quang, V. X. Luu, M. Trippenbach, R. Buczynski, Dispersion Characteristics of A Suspended-core Optical Fiber Infiltrated with Water, Applied Optics, Vol. 56, No. 4, 2017, pp. 1012-1019, https://doi.org/10.1364/AO.56.001012.

[6] D. X. Khoa, C. V. Lanh, C. V. Long, H. D. Quang, V. M. Luu, M. Trippenbach, R. Buczyński, Influence of Temperature on Dispersion Properties of Photonic Crystal Fibers Infiltrated with Water, Optical and Quantum Electronics, Vol. 49, No. 2, 2017, pp. 1-12, https://doi.org/10.1007/s11082-017-0929-3.

[7] C. V. Lanh, A. Anuszkiewicz, A. Ramaniuk, R. Kasztelanic, D. X. Khoa, M. Trippenbach, R. Buczynski, Supercontinuum Generation in Photonic Crystal Fibres with Core Filled with Toluene, Journal of Optics, Vol. 19, No. 12, 2017, pp. 125604, https://doi.org/10.1088/2040-8986/aa96bc.

[8] K. M. Hilligsoe, H. N. Paulsen, J. Thogersen, S. R. Keiding, J. J. Larsen, Initial Steps of Supercontinuum Generation in Photonic Crystal Fibers, Journal of the Optical Society of America B, Vol. 20, No. 9, 2003, pp. 1887-1893, https://doi.org/10.1364/JOSAB.20.001887.

[9] A. Medjouri, A. M. Simohamed, O. Ziane, A. Boudrioua, Analysis of A New Circular Photonic Crystal Fiber with Large Mode Area, Optik-International Journal for Light and Electron Optics, Vol. 126, No. 24, 2015, pp. 5718-5724, https://doi.org/ 10.1016/j.ijleo.2015.09.035.

[10] S. K. Pandey, Y. K. Prajapati, J. B. Maur, Design of Simple Circular Photonic Crystal Fiber Having High Negative Dispersion and Ultra-low Confinement Loss, Results in Optics, Vol. 1, 2020, pp. 100024, https://doi.org/10.1016/j.rio.2020.100024.

[11] S. Sen, M. A. A. Shafi, M. A. Kabir, Hexagonal Photonic Crystal Fiber (H-PCF) Based Optical Sensor with High Relative Sensitivity and Low Confinement Loss for Terahertz (Thz) Regime, Sensing and Bio-sensing Research, Vol. 30, 2020, pp. 100377, https://doi.org/10.1016/j.sbsr.2020.100377.

[12] Y. E. Monfared, A. R. M. M. Javan, A. R. M. Kashani, Confinement Loss in Hexagonal Lattice Photonic Crystal Fibers, Optik-International Journal for Light and Electron Optics, Vol. 124, No. 24, 2013, pp. 7049-7052, https://doi.org/10.1016/j.ijleo.2013.05.168.

[13] Y. Wang, S. Li, J. Wu, P. Yu, Z. Li, Design of an ultrabroadband and compact filter based on square-lattice photonic crystal fiber with two large gold-coated air holes, Photonics and Nanostructures - Fundamentals and Applications, Vol. 41, 2020, pp. 100816, https://doi.org/10.1016/j.photonics.2020.100816.

[14] L. T. B. Tran, N. T. Thuy, V. T. M. Ngoc, L. C. Trung, L. V. Minh, V. C. Long, D. X. Khoa, C. V. Lanh, Analysis of Dispersion Characteristics of Solid-core Pcfs with Different Types of Lattice in the Claddings, Infiltrated with Ethanol, Photonics Letters of Poland, Vol. 12, No. 24, 2020, pp. 106-108, https://doi.org/10.4302/plp.v12i4.1054.

[15] https://www.lumerical.com/products/mode **(**accessed on: December 15th, 2021).

[16] C. V. Lanh, N. T. Thuy, H. T. Duc, L. T. B. Tran, V. T. M. Ngoc, D. V. Trong, L. C. Trung, H. D. Quang, D. Q. Khoa, Comparison of Supercontinuum Spectrum Generating by Hollow Core Pcfs Filled with Nitrobenzene with Different Lattice Types, Optical and Quantum Electronics, Vol. 54, No. 5, 2022, pp. 300, https://doi.org/10.1007/s11082-022-03667-y.

[17] K. Saitoh, M. Koshiba, T. Hasegawa, E. Sasaoka, Chromatic Dispersion Control in Photonic Crystal Fibers: Application to Ultra-flattened Dispersion, Optics Express, Vol. 11, No. 8, 2003, pp. 843-852, https://doi.org/10.1364/OE.11.000843.

[18] K. Moutzouris, M. Papamichael, S. C. Betsis, I. Stavrakas, G. Hloupis, D. Triantis, Refractive, Dispersive and Thermo-optic Properties of Twelve Organic Solvents in the Visible and Near-infrared, Applied Physics B, Vol. 116, No. 3, 2014, pp. 617-622, https://doi.org/10.1007/s00340-013-5744-3.

[19] J. C. Knight, T. A. Birks, R. F. Cregan, P. S. J. Russell, Large Mode Area Photonic Crystal Fibre, Optics Photonics News, Vol. 9, No. 12, 1998, pp. 34-35, https://doi.org/10.1364/OPN.9.12.000034.

[20] J. Pniewski, T. Stefaniuk, L.V. Hieu, V. C. Long, C.V. Lanh, R. Kasztelanic, G. Stępniewski, A. Ramaniuk, M. Trippenbach, R. Buczyński, Dispersion Engineering in Nonlinear Soft Glass Photonic Crystal Fibers Infiltrated with Liquids, Applied Optics, Vol. 55, No. 19, 2016, pp. 5033-5040, https://doi.org/10.1364/AO.55.005033.